

Cooperative transport with selective kinetic constraints

Mauro Sellitto*

Dipartimento di Ingegneria, Università della Campania “Luigi Vanvitelli”,

Via Roma 29, I-81031 Aversa (CE), Italy.

The Abdus Salam International Centre for Theoretical Physics,

Strada Costiera 11, I-34151 Trieste, Italy.

(Dated: March 13, 2024)

Abstract

We introduce and study a family of cooperative exclusion processes whose microscopic dynamics is governed by selective kinetic constraints. They display, in sharp contrast to the simple symmetric exclusion process, density profiles that can be concave, convex or both, depending on the density of boundary particle reservoirs. A mean-field analysis based on a diffusion equation with a density-dependent diffusion coefficient qualitatively reproduces this behaviour, and suggests its occurrence in liquids with a diffusivity anomaly.

* mauro.sellitto@unicampania.it, mauro.sellitto@gmail.com

Introduction. – Cooperative transport underlies the variety of complex behaviours observed in soft condensed matter systems where the subtle interplay of weak entropic forces and nonequilibrium fluxes conspire to sustain highly flexible organized structures and their biological functionality [1]. While a first-principle characterization of these often counterintuitive features remains difficult, coarse grained approaches based on exclusion processes [2, 3], have been successfully applied to several problems such as polymerization kinetics on nucleic acid templates, molecular motors, and cellular transport, to name only a few [4–6]. Moreover, and perhaps more importantly, they have also come to play a paradigmatic role in recent advances of nonequilibrium statistical mechanics [6, 7].

Constrained exclusion processes, in which particle hopping requires a *minimum* number of vacant neighbours [8, 9], are already known to display rich nonequilibrium properties such as non-Fickian transport, differential negative resistance, heterogeneous dynamics, non-standard fluctuation relation, extending regimes of anomalous diffusion, dynamical free energy singularities [10–14], and systematic approaches for computing transport diffusion coefficient with increasing accuracy have been recently developed for this class of non-gradient stochastic lattice gases [15, 16].

In this paper we investigate a more general family of cooperative exclusion processes in which the number of vacant neighbours required for hopping is not determined by a minimum threshold but rather can be any specific set of non-negative integers (lower than lattice coordination number). This idea of *selective* kinetic constraints has been recently introduced in the context of bootstrap percolation to provide models of multiple hybrid phase transitions in a fully homogeneous environment [17]. We are primarily interested here in the emergence of complex convexity-change density profiles and dynamical effective particle attraction or repulsion generated by the subtle interplay of nonequilibrium fluxes and kinetic constraints, in the absence of any static interaction (apart from hard-core exclusion).

Our results show that constraining some transition probabilities to zero leads to density profiles that are globally not bounded by those obtained in the absence of constraints with the same boundary condition. As this property cannot be obviously anticipated and may appear rather paradoxical at a glance we first discuss its occurrence in the macroscopic context of a diffusion equation with a density-dependent diffusion coefficient, where it can be easily understood as a consequence of a diffusivity anomaly. Then, we see how it can be realized microscopically on a lattice and, finally, present numerical results showing that the

hydrodynamic behaviour of cooperative exclusion processes is well accounted for, at least qualitatively, by a diffusion equation in which the diffusion coefficient is naively estimated by neglecting particle correlations.

Diffusion equation. – Let us assume that the transport process occurs in a interval of size L and the system dynamics is governed by the partial differential equation:

$$\frac{\partial \rho}{\partial t} = \frac{\partial}{\partial x} \left[D(\rho) \frac{\partial \rho}{\partial x} \right], \quad (1)$$

with boundary condition $\rho(0, t) = \rho_0$ and $\rho(L, t) = \rho_1$, where $\rho(x, t)$ is the particle density at position $x \in [0, L]$ and time t , and $D(\rho)$ is the density-dependent diffusion coefficient. In the steady state the particle current:

$$J = -D(\rho) \frac{\partial \rho}{\partial x} \quad (2)$$

is uniform and constant, and the particle density profile is implicitly determined by:

$$x(\rho) = a + b \int D(\rho) d\rho, \quad (3)$$

where the constants a and b are fixed by the boundary condition $x(\rho_0) = 0$, $x(\rho_1) = L$. When the diffusion coefficient does not depend on particle density the steady state current J is proportional to $\rho_1 - \rho_0$, and the steady state density profile is linear:

$$\rho_{\text{linear}}(x) = \rho_0 + (\rho_1 - \rho_0) \frac{x}{L}. \quad (4)$$

On a lattice this situation is realised by the simple symmetric exclusion process (SSEP), in which particles interact only with hard core exclusion. When the diffusion coefficient depends on $\rho(x)$ something more interesting happens. For systems with slow dynamics, in which $D(\rho)$ monotonically decreases at high particle density, one generally observes convex density profiles, $\rho''_{\text{slow}}(x) < 0$, leading to the overall upper bound:

$$\rho_{\text{slow}}(x) < \rho_{\text{linear}}(x), \quad \forall x \in (0, L). \quad (5)$$

A simple analytically solvable instance is given by a power-law density-dependent diffusion coefficient and a lattice realisation is provided by *constrained* exclusion processes [10]. Although the relation $x'(\rho) \propto D(\rho)$ guarantees that $\rho(x)$ is always monotonic in x , the possibility of convexity-change profiles may still occur for more general forms of cooperative

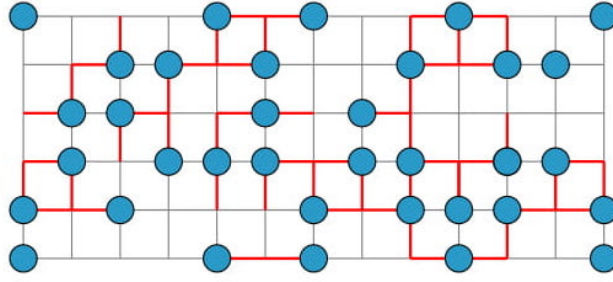


FIG. 1. Example of lattice configuration in a 2D cooperative exclusion process in which particle moves to a vacant neighbour are allowed only if the particle does not have two vacant neighbours, before and after the move. Forbidden particle hopping are denoted by red lattice bonds (full periodic boundary condition is assumed).

dynamics, and precisely in systems with a diffusivity anomaly in which relaxation dynamics becomes faster upon isothermal compression. This is the opposite of what happens in a “normal” liquid, where a reduction in the specific volume generally limits the ability of molecules to move. Such an unusual feature is shared by a number of liquids, typically with directional interactions (the most important of which being certainly water), and is manifested by a $D(\rho)$ that exhibits a minimum or a maximum in some density range (see Refs. [18–21] for some examples). Evidently, one observes a convex (concave) $\rho(x)$ when $D'(\rho) < 0$ ($D'(\rho) > 0$). In particular, there will be some boundary densities, for which $\rho(x)$ will change convexity at location $x(\rho^*)$ such that $D'(\rho^*) = 0$. In this case, no global inequality like Eq. (5) can be stated. The key question is to identify the conditions on microscopic transition probabilities under which such unusual features arise in the absence of static interactions.

Microscopic models. – We argue that the family of cooperative exclusion processes (CEP) we now introduce features convexity-change density profiles when kinetic constraints are of selective type. Selective here means that particle hopping requires some specific numbers of vacant neighbours before and after the move, rather than a minimum threshold m , as in usual kinetically constrained models (KCM) [9]. When constraints act selectively in an intermediate range of density, or also at both low and high densities, we expect that the diffusion coefficient is not monotonic (i.e., it exhibits a minimum or a maximum,

respectively). One can give a useful mean-field estimation for CEP diffusion coefficient by neglecting correlations between nearby particles, in terms of the probability of not having certain numbers of vacant neighbours before and after the move, just as done for KCM [14–16]:

$$D_{\mathcal{S}}^{\text{NC}}(\rho) = \left[1 - \sum_{i \in \mathcal{S}} \binom{c-1}{i} \rho^{c-1-i} (1-\rho)^i \right]^2, \quad (6)$$

where c is the lattice coordination number and \mathcal{S} is the non-negative integer sequence representing the numbers of vacant neighbours (not counting the departure and target site, before and after the move, respectively) for which a particle move is *not* allowed. In the above no-correlation (NC) approximation, binomial terms account for the multiplicity of possible configurations of particles and vacancies, around the departure and target site, that prevent hopping, and the power 2 comes from the detailed balance condition. When the integer sequence \mathcal{S} is gapless, i.e., $\mathcal{S} = \{0, 1, 2, \dots, m-2\}$, the usual *cumulative* form of kinetic constraints is recovered (in which a move is allowed only when the particle has at least $m-1$ vacant sites, not counting the departure and target site, before and after the move, respectively), and the diffusion coefficient decreases monotonically all the way down to $\rho = 1$. When there are gaps in \mathcal{S} , e.g., when the sum over \mathcal{S} in Eq. (6) includes only terms in $\rho^j(1-\rho)^k$ (with nonzero j and k), or both terms ρ^{c-1} and $(1-\rho)^{c-1}$, the diffusion coefficient may exhibit extrema in an intermediate range of density. In analogy with its cumulative counterpart, and consistently with Ref. [16], we expect that Eq. (6) yields a general upper bound for the actual diffusion coefficient, which can be obtained to the lowest order approximation from a variational principle due to Varadhan [22].

Numerical results. – To substantiate our claim more concretely we now consider an exclusion process on a two dimensional square lattice in which a particle move to a nearby empty site occurs only when the particle does not have two vacant neighbours, before and after the move. In the previously introduced classification scheme (which does not take into account the departure and target sites) this corresponds to $\mathcal{S} = \{1\}$. A representative example of disallowed moves is shown by red bonds in the particle configuration of Fig. 1. Dynamics with the above selective constraint obeys detailed balance and equilibrium measure is trivial just as in any other KCM of glassy dynamics [8, 9]. In the limit of very low and very high particle density the selective kinetic constraint plays no role and the standard

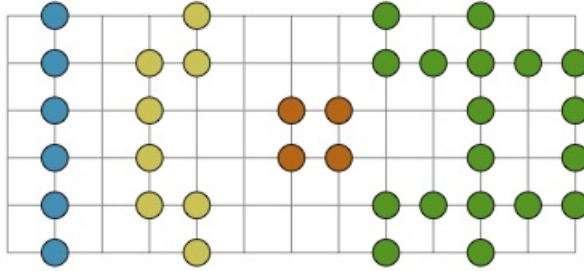


FIG. 2. Four examples of metastable particle clusters (each with a different colour) that are permanently frozen as long as they remain isolated (periodic boundary condition in the vertical direction). The selective constraint allows for a particle move only if the particle does not have two vacant neighbours, before and after the move.

SSEP is recovered. In the intermediate range of density dynamics becomes weakly cooperative. In fact, particle rearrangements occur rather quickly and, although there exist particle configurations which are permanently frozen as long as they remain completely isolated (see Fig. 2 for some examples), their lifetime is actually quite short: as soon as a single particle comes close to their border the metastable structure breaks up relatively faster. This leads to a dynamics that is ergodic at any density. We have explicitly checked, for an equilibrium system with fixed particle number, that the mean-square displacement is normal after a very short transient and no anomalous diffusion is observed on extended time scales.

We have performed Monte Carlo simulation of the nonequilibrium steady state attained by the system when it is coupled to particle reservoirs at its edges. The system consists of a square lattice of size $L \times 2L$ with periodic boundary conditions in all directions in order to avoid spurious edge effects due to the kinetic constraint. This amounts to running two independent bulk systems sharing the same reservoirs, one located at $z = L$ (reservoir with density ρ_1) and the other at $z = 0$ (reservoir with density ρ_0). Numerical results for local density profiles are averaged over 10^6 independent configurations and have been compared with the inverse function of density profile:

$$x(\rho) = a + b \left(\rho - 2\rho^3 + \frac{3}{2}\rho^4 + \frac{9}{5}\rho^5 - 3\rho^6 + \frac{9}{7}\rho^7 \right) \quad (7)$$

(with constants a and b fixed by boundary condition), which is obtained exactly from Eq. (3)

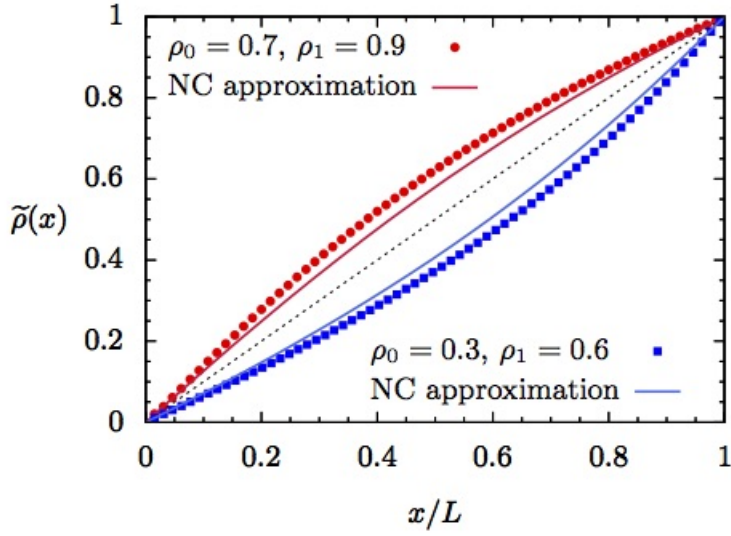


FIG. 3. Normalised density profiles. Square and circle symbols denote numerical simulations data, solid lines correspond to no-correlation (NC) approximation. The straight dotted line is the SSEP reference profile.

in the no-correlation approximation for the diffusion coefficient:

$$D_1^{\text{NC}}(\rho) = [1 - 3\rho^2(1 - \rho)]^2. \quad (8)$$

This function has a minimum at $\rho^* = 2/3$. According to our analysis of diffusion equation, this means that one should observe globally convex or concave profiles depending on whether ρ_0 and ρ_1 are both smaller or larger than ρ^* , respectively. Or also, a density profile that changes convexity at position $x(\rho^*)$ when $\rho_0 < \rho^* < \rho_1$. For the sake of simplicity we use the normalised density profile $\tilde{\rho}(x)$ defined as:

$$\tilde{\rho}(x) \equiv \frac{\rho(x) - \rho_0}{\rho_1 - \rho_0}. \quad (9)$$

Figure 3 shows the numerical results for $\rho_0 = 0.3, \rho_1 = 0.6$ and $\rho_0 = 0.7, \rho_1 = 0.9$ for a system of linear size $L = 128$ (the absence of finite-size effects has been checked with $L = 64$ and $L = 256$). In contrast with the boundary-driven KA model [10, 15], we observe convex profiles for large values of reservoirs density, and concave ones when ρ_0, ρ_1 are both smaller than ρ^* . The comparison with analytical predictions of the diffusion equation obtained in the NC approximation (full lines in Fig. 3) shows that discrepancies are rather mild, as also observed in Ref. [15] for the KA model.

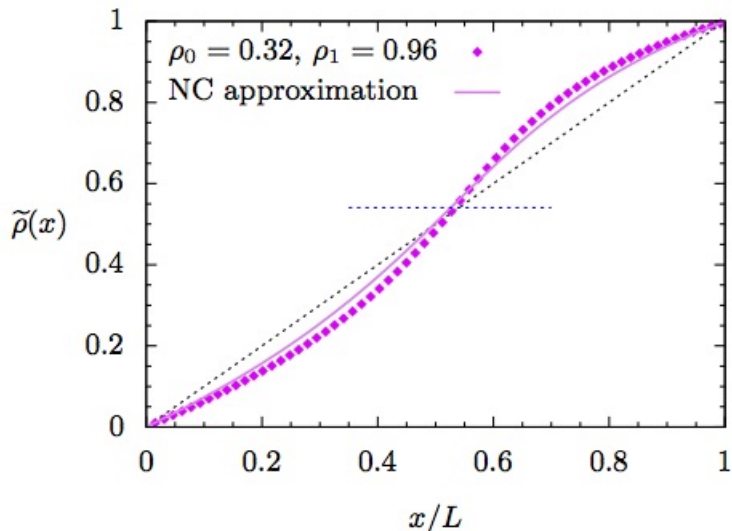


FIG. 4. Convex-to-concave crossover normalised density profiles. Symbols denote numerical simulations data, the solid line correspond to the no-correlation (NC) approximation. The horizontal segment locates the estimated $\rho^* = 2/3$ (corresponding to $\tilde{\rho}^* \simeq 0.54\dots$) in the NC approximation. (The straight dotted line is the reference SSEP profile).

Figure 4 shows a convexity-change density profile obtained for $\rho_0 < \rho^* < \rho_1$, that is $\rho_0 = 0.32$, $\rho_1 = 0.96$. Also in this case we see that predictions are well confirmed, in particular the position at which convexity changes. A more refined approximation scheme can be certainly obtained by exploiting the systematic approaches recently developed in Refs. [15, 16]. We leave this to future works. What we would like to emphasize here is the rather unusual nature of density profiles we have obtained. Even though, from a microscopic point of view, there is evidently no *static* force, the overall effect of disallowing some moves and imposing a current flux in the system favours those kinetic paths that bring particles closer or farther, as they travel from the high to the low density reservoirs. This suggests that the interplay of nonequilibrium drive and kinetic constraints leads to the emergence of effective dynamical interactions, which may be attractive or repulsive depending on the sign of $D'(\rho)$ and are manifested in convex, concave or convexity-change density profiles. Perhaps surprisingly, *transverse* local density fluctuations are not affected by the shape of density profiles and turns out to be always uncorrelated (for sufficiently large system size),

irrespective of the boundary driving force, just as in SSEP:

$$L [\langle \rho(x)^2 \rangle - \langle \rho(x) \rangle^2] = \langle \rho(x) \rangle (1 - \langle \rho(x) \rangle). \quad (10)$$

This is shown in the parametric plot of Fig. 5.

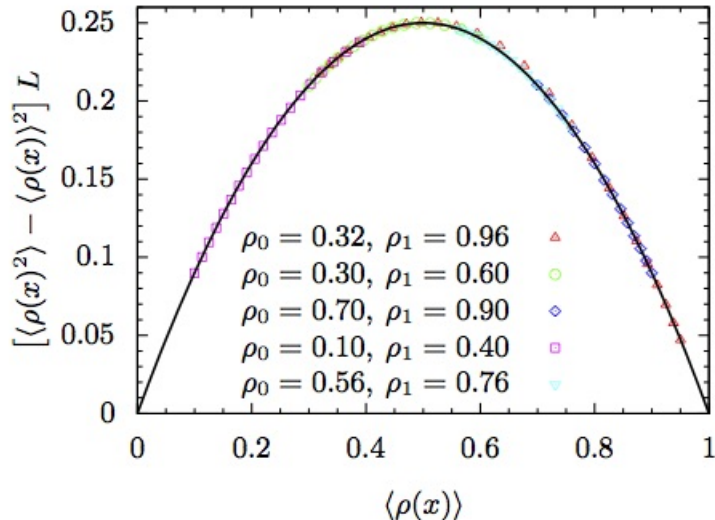


FIG. 5. Parametric plot of transverse density fluctuations vs density profile for several values of reservoir density, ρ_0 and ρ_1 , and linear system size $L = 128$. The solid line is the result expected from uncorrelated SSEP-like transverse fluctuations.

We have carried out the same analysis for another cooperative exclusion process on a square lattice, in which a particle move is allowed only when the particle does not have one or four vacant neighbours, before and after the move. In our classification scheme this is represented by the selective constraint $\mathcal{S} = \{0, 3\}$, which corresponds to the particle-hole symmetry invariant analog of the 2D KA model [8]. On a Bethe lattice it has two glass transition critical points (at low and high density, related by the particle-hole symmetry). On a square lattice an argument similar to that developed in [23] ensures that dynamics is ergodic at any density, even though it is strongly cooperative and sluggish when $\rho \rightarrow 0$ or $\rho \rightarrow 1$ (diffusion becoming singular near these points). The NC approximation for the diffusion coefficient in this case is:

$$D_{0,3}^{\text{NC}}(\rho) = [1 - \rho^3 - (1 - \rho)^3]^2, \quad (11)$$

which has a maximum at $\rho^* = 1/2$. This gives profile shapes that are just the opposite of those discussed previously for the case $\mathcal{S} = \{1\}$, i.e., concavity for $\rho_0 < 1/2$, $\rho_1 < 1/2$,

convexity for $\rho_0 > 1/2$, $\rho_1 > 1/2$, and convexity-change profiles for $\rho_0 < 1/2 < \rho_1$. The comparison with Monte Carlo results shows that these predictions are well reproduced with small discrepancies and improving accuracy as ρ_0 and ρ_1 increasingly depart from 0 and 1. Thus, we conclude that the properties discussed above are quite general of the CEP family and, in spite of substantial particle correlation arising from cooperative dynamics, the hydrodynamic behaviour is well captured, at least qualitative, by the nonlinear diffusion equation. More exotic features, like density profiles with multiple changes of convexity, can also be observed provided that the system has a larger lattice coordination number and extra gaps in \mathcal{S} , as suggested by Eq. (6), but we have not explored this further.

Conclusions – In summary, we have shown that cooperative exclusion processes with selective kinetic constraints and trivial equilibrium properties, display density profiles with a considerable rich structure in the absence of any static interaction. Such features are the macroscopic nonequilibrium manifestation of attractive and repulsive statistical forces that arise from microscopically constrained current-carrying nonequilibrium steady states. This is nicely captured by a diffusion equation with an approximated density-dependent diffusion coefficient that neglects particle correlations. Quite independently of the nature of kinetic constraints, which must be considered as a coarse-grained description of the real microscopic dynamics, the analysis of the diffusion equation shows that convexity-change profiles are intimately related to a non-monotonic density-dependent diffusion coefficient. Therefore, liquids with a diffusivity anomaly and soft matter systems with a reentrant dynamics [18–21] are the most suitable candidates in which the above predictions can be tested.

-
- [1] P. Nelson, *Biological Physics* (New York: WH Freeman, 2004).
 - [2] A.L. Hodgkin and R. D. Keynes, *The Journal of Physiology* **128**, 61 (1955).
 - [3] J.T. MacDonald, J.H. Gibbs and A. Pipkin, *Biopolymers* **6**, 1 (1968).
 - [4] P.L. Krapivsky, S. Redner, and E. Ben-Naim, *A Kinetic View of Statistical Physics*, (Cambridge: Cambridge University Press, 2010).
 - [5] A. Schadschneider, D. Chowdhury, and K. Nishinari, *Stochastic Transport in Complex Systems: From Molecules to Vehicles* (Amsterdam: Elsevier, 2011).
 - [6] T. Chou, K. Mallick and R.K.P. Zia, *Rep. Prog. Phys.* **74**, 116601 (2011).

- [7] B. Derrida, *J. Stat. Mech.* P07023 (2007).
- [8] W. Kob and H.C. Andersen, *Phys. Rev. E* **48**, 4364 (1993).
- [9] For a review, see: F. Ritort and P. Sollich, *Adv. Phys.* **52**, 219 (2003).
- [10] M. Sellitto, *Phys. Rev. E* **65**, 020101(R) (2002).
- [11] M. Sellitto, *Phys. Rev. Lett.* **101**, 048301 (2008).
- [12] M. Sellitto, *Phys. Rev. E* **80**, 011134 (2009).
- [13] F. Turci and E. Pitard, *Europhys. Lett.* **94**, 10003 (2011).
- [14] F. Turci, E. Pitard, and M. Sellitto, *Phys. Rev. E* **86**, 031112 (2012).
- [15] E. Teomy and Y. Shokef, *Phys. Rev. E* **95**, 022124 (2017).
- [16] C. Arita, P.L. Krapivsky, and K. Mallick, *J. Phys. A: Math. Theor.* **51**, 125002 (2018).
- [17] M. Sellitto, to appear on *J. Stat. Mech.* (2019).
- [18] F.W. Starr, F. Sciortino, and H.E. Stanley, *Phys. Rev. E* **60**, 6757 (1999).
- [19] M.C. Rechtsman, F.H. Stillinger, and S. Torquato, *J. Phys. Chem. A* **111**, 12816 (2007).
- [20] L. Berthier, A.J. Moreno, and G. Szamel, *Phys. Rev. E* **82**, 060501(R) (2010).
- [21] M. Pica Ciamarra and P. Sollich, *J. Chem. Phys.* **138**, 12A529 (2013).
- [22] H. Spohn, *Large Scale Dynamics of Interacting Particles* (Heidelberg: Springer-Verlag, 1991).
- [23] C. Toninelli, G. Biroli, and D.S. Fisher, *J. Stat. Phys.* **120**, 167 (2005).